Electronic effect of lead substitution in single-crystal Bi(Pb)-Sr-Ca-Cu-O superconductors determined by scanning tunneling microscopy

Zhe Zhang, Yue Li Wang, Xian Liang Wu, Jin-Lin Huang, and Charles M. Lieber
Department of Chemistry, Columbia University, New York, New York 10027
(Received 14 February 1990; revised manuscript received 24 April 1990)

Scanning tunneling microscopy has been used to characterize directly the surface electronic structure of a series of single-crystal $Pb_xBi_{2-x}Sr_2CaCu_2O_8$ superconductors. High-resolution spectroscopic measurements show that within ± 0.5 eV of the Fermi level the Bi(Pb)-O electronic structure is independent of the Pb concentration $(x \leq 0.7)$. Extended spectroscopic measurements demonstrate that the density of unfilled states at $+1$ eV systematically decrease as the concentration of Pb increases, although the filled states between 0 and -2 eV are essentially independent of the concentration of Pb. In addition, analysis of the differential conductivity indicates that the surface conductivity varies from weakly metallic to semiconducting as the tip-surface separation increases.

Substitutional doping of metals in high-temperature superconductors has been employed extensively in attempts to elucidate and improve the superconducting properties of these materials. For example, since Sunshine *et al.*[1] reported that Pb substitution in the Bi-Sr-Ca-Cu-O system enhanced the onset of superconductivity from 84 to 107 K numerous studies of these Pb-substituted materials have been reported.[2-9] In polycrystalline $(BiPb)_2Sr_2Ca_{n-1}Cu_nO_{2n+4}$ materials Pb substitution has been found to enhance the formation of the $n=3$ (110 K) phase versus the $n=2$ (85 K) phase,[2,6] although the lattice parameters and transition temperatures (T_c) for a given phase do not vary substantially.[5,6] In addition, electron-diffraction,[2-4] x-ray-diffraction,[5,6] and scanning-tunneling-microscopy[9] studies have shown that the strong one-dimensional superstructure observed in $Bi_2Sr_2CaCu_2O_8$ changes with Pb substitution. In contrast, few studies have been reported that address the electronic structure of these Pb-substituted materials[10] and hence it is not known whether Pb perturbs the electronic states important for superconductivity in this system.

To probe directly the effect of Pb substitution on the normal-state density of states we have used scanning tunneling microscopy (STM), and herein we report the first systematic room-temperature tunneling measurements for single-crystal $Pb_xBi_{2-x}Sr_2CaCu_2O_8$ $(x=0, 0.3,$ and 0.7) materials. STM is an ideal technique for characterizing the electronic effects of Pb substitution since Pb replaces Bi in the Bi-O layers,[7,8] and $Pb_xBi_{2-x}Sr_2CaCu_2O_8$ crystals can be cleaved to expose a Bi(Pb)-O plane at the sample surface. Recently, two ultrahigh-vacuum (UHV) STM studies of the electronic properties of unsubstituted $Bi_2Sr_2CaCu_2O_8$ single crystals have been reported.[11,12] The conclusion of these investigations was that the Bi-O layer is nonmetallic and thus that the distinct Fermi edge observed by photoemission spectroscopy and inverse photoemission spectroscopy (IPES) is due to states in the CuO_2 planes. In this communication we will discuss our new studies of the electronic structure of the Bi(Pb)-O layer as a function of the Pb concentration. We find that there is an incomplete gap in the density of states within

± 0.5 eV of the Fermi level for the $x(Pb) =0, 0.3,$ and 0.7 samples. The finite-state density detected at the Fermi level contrasts previous STM reports.[11,12] In addition, this study demonstrates that there is a systematic decrease in the empty electronic states 1 eV above the Fermi level as $x(Pb)$ increases. These STM data together with measurements of the superconducting transition temperature are used to assess the intrinsic electronic role of Pb in the $Pb_xBi_{2-x}Sr_2CaCu_2O_8$ materials.

The single-crystal samples of $Pb_xBi_{2-x}Sr_2CaCu_2O_8$ $(x=0, 0.3, 0.7)$ were grown from Cu-O rich melts. Bulk analysis and surface analysis (Auger-electron spectroscopy) demonstrate that Pb is incorporated into these crystals at close to the Pb/Bi stoichiometry of the melts. Although the Sr and Ca concentrations are slightly deficient in these crystals, the materials will be denoted by the ideal $Pb_xBi_{2-x}Sr_2CaCu_2O_8$ formula. Single-crystal x-ray diffraction investigations of the Pb-substituted materials also show that the structures of the $x(Pb) =0, 0.3, 0.7$ materials are the same in agreement with previous reports.[5,6] Details of the synthesis and characterization of these single-crystal materials will be reported elsewhere.[13] The values of the critical temperature T_c (zero resistance) determined from dc four-point probe measurements were $85 \pm 4, 88 \pm 3,$ and 85 ± 2 K for the $x(Pb) =0, 0.3,$ and 0.7 samples, respectively (Fig. 1). In addition, magnetic measurements (Meissner effect) demonstrate that the superconducting fractions of the $x(Pb) =0-0.7$ samples are similar.

The STM measurements were made with a modified commercial instrument (Nanoscope, Digital Instruments, Inc., Santa Barbara, CA) operated in an argon-filled glove box equipped with a purification system that reduced the concentrations of H_2O and O_2 to below 1 ppm.[14] Reproducible and stable $(\geq 3$ h) STM measurements were obtained from *in situ* cleaved samples using this setup. The glove box environment $(\approx 10^{-3}$ torr $O_2)$ was used to reduce the possibility of oxygen loss from the surface of the materials that may occur in ultrahigh vacuum.[15,16] The current (I) versus voltage (V) data were acquired by interrupting the STM feedback loop, and then
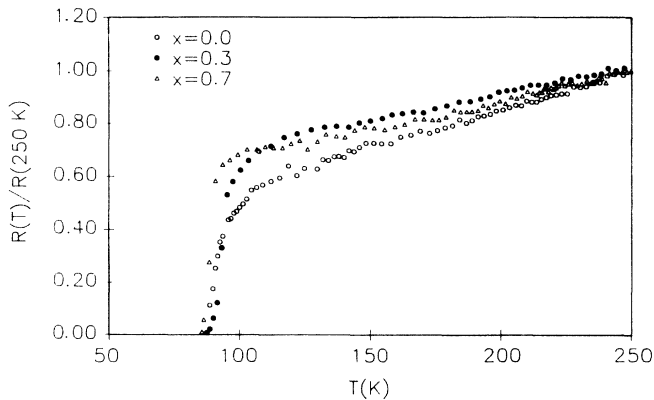
FIG. 1. Representative normalized resistivity curves for x(Pb) $=0$, 0.3, and 0.7 single-crystal samples.

the sample-tip bias voltage while digitally storing the resulting changes in the tunneling current.[17] The I-V data shown are the average of 20 to 40 curves obtained at a selected surface site; however, these measurements likely represent an average over several atomic positions due to drifts during data acquisition.

The electronic states close to the Fermi level of the Bi(Pb)-O surfaces were probed first with high-resolution measurements since these states should have the greatest influence on superconductivity. I-V curves recorded between -400 and $+400$ mV on x(Pb) $=0$, 0.3, and 0.7 single crystals are shown in Fig. 2. STM images shown as insets in Fig. 2 indicate that the observed atomic structure (period $=3.7 \pm 0.2$, 3.8 ± 0.2, and 3.7 ± 0.1, respectively) is not perturbed significantly by the incorporation of Pb into the lattice. The surface structure of these materials will be discussed in detail elsewhere.[9] The differential conductivity curves determined numerically from these I-V data are also shown in Fig. 2. The values of dI/dV increase at a similar rate as $|V|$ increases for the three spectra; furthermore, similar dI/dV curves were obtained reproducibly with our experimental setup under stable imaging conditions. In addition, these curves appear to show a gap in the density of states as suggested by two recent STM studies of the x(Pb) $=0$ material.[11,12] However, the average values of $dI/dV \pm 1\sigma$ at $V=0$ for the x(Pb) $=0$, 0.3, and 0.7 materials are 1.6 ± 0.2, 1.5 ± 0.4, and 1.6 ± 0.2 nA/V, respectively, when the feedback stabilized gap resistance is 10^8 Ω. These finite (albeit small) values for the conductivity at $V=0$ indicate that the Bi(Pb)-O layer is weakly metallic and not semiconducting.[11,12] The differential conductivity at $V=0$ determined for MoS$_2$ (a known semiconductor) using similar instrumental parameters is ca. 100 times smaller than the values obtained for the Pb$_x$Bi$_{2-x}$Sr$_2$CaCu$_2$O$_8$ materials. Hence, we believe that the observed finite conductivities are intrinsic to these materials and not due to experimental artifacts. The observation of a nonmetallic Bi-O layer in previous ultrahigh vacuum (UHV) STM studies of the parent Bi$_2$Sr$_2$Ca-Cu$_2$O$_8$ material[11,12] could be due to several factors. First, oxygen may be lost in vacuum to yield an insulating surface.[15,16] Recent UHV electron-energy-loss measurements support this suggestion since it was found that the
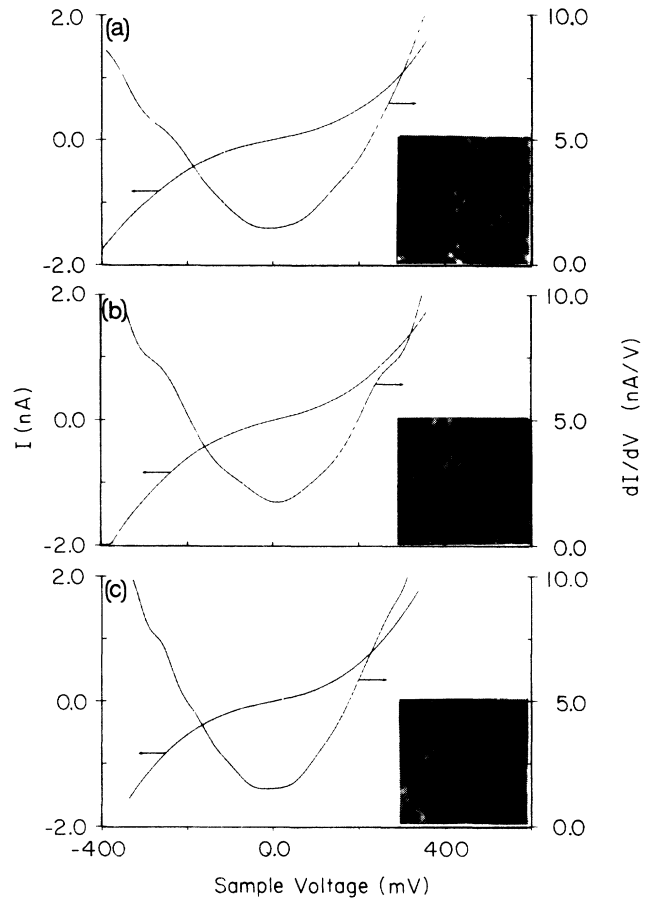

FIG. 2. Plots of I vs V and dI/dV vs V for x(Pb) $=0$, 0.3, and 0.7 materials are shown in (a), (b), and (c), respectively. These data were obtained using a feedback-stabilized tunneling gap resistance of 10^8 Ω. 40×40-Å^2 top-view atomic resolution STM images obtained in the constant current mode are shown as insets in these figures.

surface resistivity increases with time in vacuum.[16] Alternatively, we note that our high-resolution measurements were made at a closer tip sample separation than the UHV studies, and thus, the decay of the electronic states into the tunneling gap may also affect these results (see below).

To address further the metallic/nonmetallic nature of the surface layer and to determine the electronic states affected by Pb substitution we have extended the range of the I-V measurements. These data are plotted as the normalized conductivity, $(V/I)dI/dV$, since it has been well documented by Feenstra, Stroscio, and Fein[18] that $(V/I)dI/dV$ is proportional to the local density of states at the sample surface. Typical $(V/I)dI/dV$ spectra recorded between -2 and $+2$ V with a feedback stabilized gap resistance of 10^9 Ω for the x(Pb) $=0$, 0.3, and 0.7 crystals are shown in Fig. 3. In general, reproducible data was recorded for stable imaging conditions. Between -0.6 and $+0.5$ V the three spectra exhibit similar and repeatable features that are independent of x(Pb). These features include a peak in the density of states at -0.5 to -0.6 eV, a peak at 0.4 to 0.5 eV, and a low-state density be-
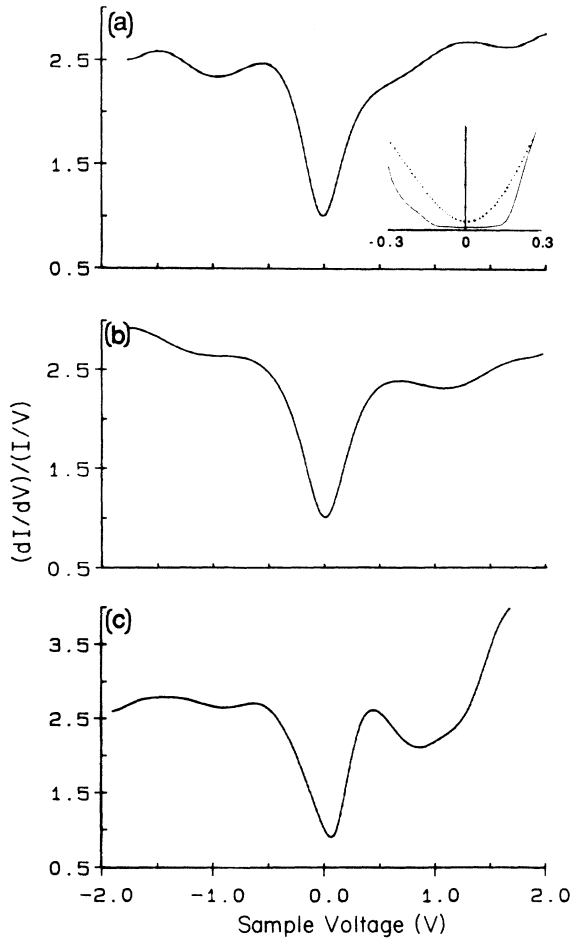
FIG. 3. Plots of the normalized conductivity vs sample voltage for the x(Pb) $=0$, 0.3, and 0.7 materials are shown in (a), (b), and (c), respectively. The voltage corresponds to the energy relative to the Fermi level ($V=0$). The inset in (a) shows dI/dV vs V (volts) curves for data recorded with a gap resistance of 10^8 Ω ($\cdots$) and 10^9 Ω (——). The density of states at $+1$ V systematically decrease [curves (a)-(c)] as the concentration of Pb increases.

tween these two peaks. In the inset to Fig. 3(a) we have also directly compared the differential conductivity for the extended range and high-resolution data in this region. Notably, we find (after scaling for the exponential distance dependence of the tunneling current) that there is a significantly larger gap in the 10^9 Ω versus the 10^8 Ω data. We therefore conclude that the tip-sample separation plays an important role in determining our sensitivity to the electronic states.[19] One possible explanation for this interesting observation is that the finite density of

states at $V=0$ associated with the metallic Cu-O layer contributes increasingly to the tunneling current as the tip is brought closer to the surface (i.e., at a lower gap resistance), although additional work will be needed to fully understand this phenomenon.

In addition, there are significant and reproducible differences in the electronic structure at energies further removed from the Fermi level. In particular, as the concentration of Pb in the Bi(Pb)-O layers increases we observe a systematic decrease in the unfilled states 1 eV above the Fermi level. The filled states are, however, essentially unperturbed by Pb substitution from 0 to -2 eV within the resolution of our experiments. To understand the origin or the systematic decrease in the electronic states at $+1$ eV we consider the electronic structure of $Bi_2Sr_2Ca-Cu_2O_8$. Recent IPES (Refs. 10, 20, and 21) and theoretical[22] studies of $Bi_2Sr_2CaCu_2O_8$ indicate that the Bi-$6p$ band lies ≥ 1 eV above the Fermi level, while O-$2p$ states contribute predominantly to the density of states near the Fermi level. It is thus likely that the reduction in the density of states that we observe at $+1$ eV is due to a decrease in the density of Bi-$6p$ states as the concentration of Pb increases. Alternatively, differences in the Pb-O vs Bi-O bonding could change the energy dependence of the O-$2p$ band. Regardless of the exact origin of the observed decrease in the density of states as x(Pb) increases, it is important to recognize that T_c is essentially independent of the concentration of Pb ($x \leq 0.7$) (Fig. 1). Hence, we suggest that this variation in the electronic structure is sufficiently far removed from the Fermi level that it does not perturb the Cu-O electronic states essential for superconductivity.

In summary, we have used STM to probe the local electronic structure of a series of single-crystal Pb-substituted Bi-Sr-Ca-Cu oxide materials at room temperature. High-resolution spectroscopic tunneling measurements demonstrate that near the Fermi level the density of states are nearly independent of the level of Pb substitution. Extended spectroscopic measurements further show that the density of unfilled electronic states at $+1$ eV systematically decreases as the concentration of Pb increases, although the filled states between 0 and -2 eV are essentially independent of the concentration of Pb. In addition, analysis of the differential conductivity indicates that the apparent surface conductivity varies from weakly metallic to semiconducting as the tip surface separation increases.

[1]S. A. Sunshine *et al.*, Phys. Rev. B **38**, 893 (1988).

[2]R. Ramesh, G. Thomas, S. Green, C. Jiang, Y. Mei, M. L. Rudee, and H. L. Luo, Phys. Rev. B **38**, 7070 (1988).

[3]C. H. Chen, D. J. Werder, G. P. Espinosa, and S. A. Cooper, Phys. Rev. B **39**, 4686 (1989).

[4]P. Bordet, J. J. Capponi, C. Chaillout, J. Chenavas, A. W. Hewat, E. A. Hewat, J. L. Hodeau, and M. Marezio, Stud. High Temp. Supercond. **2**, 171 (1989).

[5]J. Schneck, L. Pierre, J. C. Toledano, and C. Daguet, Phys. Rev. B **39**, 9624 (1989).

[6]S. X. Dou, H. K. Liu, A. J. Bourdillon, M. Kviz, N. X. Tan, and C. C. Sorrell, Phys. Rev. B **40**, 5266 (1989).

[7]R. Ramesh, M. S. Hegde, C. C. Chang, J. M. Tarascon, S. M. Green, and H. L. Luo, J. Appl. Phys. **66**, 4878 (1989).

[8]H. Nobumasa, T. Arima, K. Shimizu, Y. Otsuka, Y. Murata, and T. Kawai, Jpn. J. Appl. Phys. **28**, L57 (1989).

[9]X. L. Wu, Z. Zhang, Y. L. Wang, and C. M. Lieber, Science (to be published).

[10]T. J. Wagener, Y. Hu, Y. Gao, M. B. Jost, J. H. Weaver, N. D. Spencer, and K. C. Goretta, Phys. Rev. B **39**, 2928 (1989).

[11]M. Tanaka *et al.*, Nature (London) **339**, 691 (1989).

[12]C. K. Shih, R. M. Feenstra, J. R. Kirtley, and G. V. Chandrashekhar, Phys. Rev. B **40**, 2682 (1989).

[13]Y. L. Wang and C. M. Lieber (unpublished).

[14]S. P. Kelty and C. M. Leiber, Phys. Rev. B **40**, 5856 (1989).

[15]N. Miura, H. Suzuta, Y. Deshimaru, Y. Shimizu, H. Sakashita, and N. Yamazoe, Jpn. J. Appl. Phys. **28**, L1112 (1989).

[16]J. E. Demuth, B. N. J. Persson, F. Holtzberg, and C. V. Chadrashekhar, Phys. Rev. Lett. **64**, 603 (1990).

[17]R. M. Tromp, R. J. Hamers, and J. E. Demuth, Science **234**, 304 (1986).

[18]R. M. Feenstra, J. A. Stroscio, and A. P. Fein, Surf. Sci. **181**, 295 (1987).

[19]Measurements of dI/ds (s = tip sample separation) show that the enhanced conductivity at $V = 0$ for the data obtained with a gap resistance of 10^8 Ω is not due to tip surface contact. However, when the gap resistance is $\leq 10^7$ Ω dI/ds exhibits behavior indicative of a strong tip sample interaction. In addition, dI/ds is nearly the same for both the 10^8- and 10^9-Ω data; this indicates that the tunneling barrier heights are similar at these two tip sample separations.

[20]W. Drube, F. J. Himpsel, G. V. Chandrashekhar, and M. W. Shafer, Phys. Rev. B **39**, 7328 (1989).

[21]R. Claessen, R. Manzke, H. Carstensen, B. Burandt, T. Buslaps, M. Skibowski, and J. Fink, Phys. Rev. B **39**, 7316 (1989).

[22]J. Ren, D. Jung, M. H. Wangbo, J. M. Tarascon, Y. Le Page, W. R. McKinnon, and C. C. Torardi, Physica C **158**, 501 (1989).
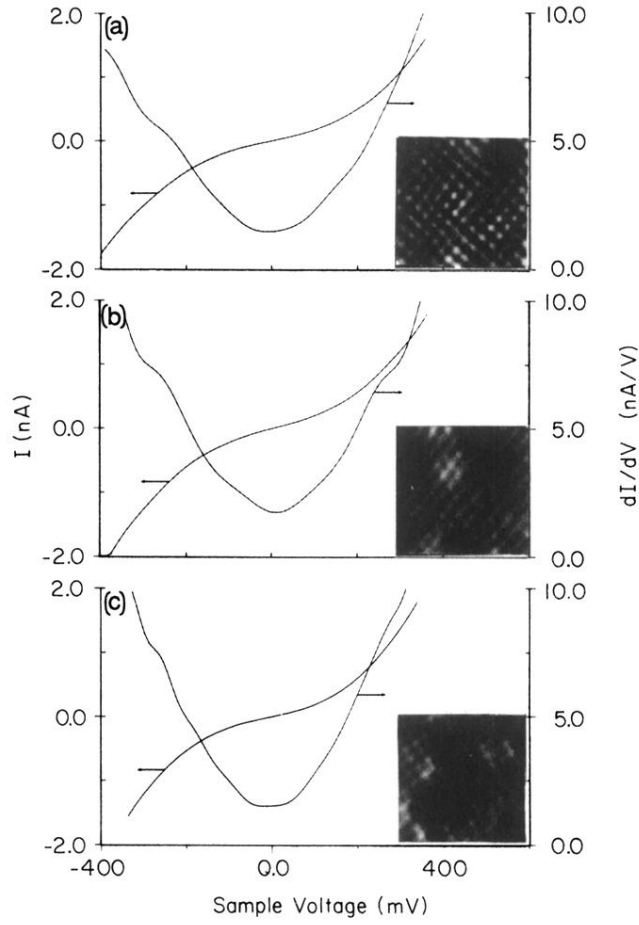
FIG. 2. Plots of *I* vs *V* and *dI/dV* vs *V* for $x(Pb) = 0$, 0.3, and 0.7 materials are shown in (a), (b), and (c), respectively. These data were obtained using a feedback-stabilized tunneling gap resistance of 10^8 Ω. 40×40-Å^2 top-view atomic resolution STM images obtained in the constant current mode are shown as insets in these figures.